

Wettability and contact angle affect precorneal retention and pharmacodynamic behavior of microspheres

Hanyu Liu^{a*}, Xinyue Han^{a*}, Huamei Li^a, Qi Tao^b, Jie Hu^a, Shuo Liu^a, Huaixin Liu^a, Jun Zhou^c, Wei Li^d, Fan Yang^a, Qineng Ping^e, Shijie Wei^a, Hongmei Liu^b, Huaqing Lin^a and Dongzhi Hou^a

^aGuangdong Engineering and Technology Research Center of Topical Precise Drug Delivery System, College of Pharmacy, Guangdong Pharmaceutical University, Guangzhou, China; ^bCAS Key Laboratory of Mineralogy and Metallogeny & Guangdong Provincial Key Laboratory of Mineral Physics and Materials, Guangzhou Institute of Geochemistry, Chinese Academy of Sciences (CAS), Guangzhou, China; ^cDepartment of English Language and Literature, University College London, London, UK; ^dGuangzhou Institute For Drug Control, Guangzhou, China; ^eCollege of Pharmacy, China Pharmaceutical University, Nanjing, China

ABSTRACT

In the present study, we describe the development of betaxolol hydrochloride and montmorillonite with ion exchange in a single formulation to create a novel micro-interactive dual-functioning sustained-release delivery system (MIDFDS) for the treatment of glaucoma. Betaxolol hydrochloride molecule was loaded onto the montmorillonite by ion exchange and MIDFDS formation was confirmed by XPS data. MIDFDS showed similar physicochemical properties to those of Betoptic, such as particle size, pH, osmotic pressure, and rheological properties. Nevertheless, the microdialysis and intraocular pressure test revealed better *in vivo* performance of MIDFDS, such as pharmacokinetics and pharmacodynamics. With regards to wettability, MIDFDS had a larger contact angle ($54.66 \pm 5.35^\circ$) than Betoptic ($36.68 \pm 1.77^\circ$), enabling the MIDFDS (2.93 s) to spread slower on the cornea than Betoptic (2.50 s). Moderate spreading behavior and oppositely charged electrostatic micro-interactions had a comprehensive influence on micro-interactions with the tear film residue, resulting in a longer precorneal retention time. Furthermore, MIDFDS had a significant sustained-release effect, with complete release near the cornea. The dual-functioning sustained-release carrier together with prolonged pre-corneal retention time (80 min) provided sufficiently high drug concentrations in the aqueous humor to achieve a more stable and long-term IOP reduction for 10 h. In addition, cytotoxicity and hemolysis tests showed that MIDFDS had better biocompatibility than Betoptic. The dual-functioning microspheres presented in this study provide the possibility for improved compliance due to low cytotoxicity and hemolysis, which suggests promising clinical implications.

ARTICLE HISTORY

Received 14 July 2021
Revised 26 August 2021
Accepted 30 August 2021



KEYWORDS

Glaucoma; montmorillonite; Eudragit; microsphere; contact angle

1. Introduction

Glaucoma, a multifactorial neurodegenerative disease characterized by retinal ganglion cell (RGC) death and degeneration of nerve axons (Delplace et al., 2015), is one of the leading causes of irreversible blindness worldwide (Kumarasamy et al., 2006; Arranz-Romera et al., 2019). Intraocular pressure (IOP) is the main clinically modifiable risk factor (Tham et al., 2014; Actis et al., 2016; O'Callaghan et al., 2017) and is often regulated by reducing humor aqueous production or increasing outflow (Geyer & Levo, 2020). The current methods used to treat glaucoma are mainly drug therapy, laser therapy, and clinical surgery (Cohen et al., 2014), among which medication is the first choice (Geyer et al., 1995; Ameeruzzafar et al., 2018). For ocular diseases, systemic administration is usually ineffective due to the presence of the blood-ocular barrier (Amo & Urtti, 2008). Therefore, topical drug delivery is considered the most appropriate treatment (Geyer et al.,

1995). Although the eye is very vulnerable to external invasive materials, it is a fairly isolated organ with several barriers, such as the tear film barrier, nodes and desmosomes of corneal epithelial cells, iris barrier, blood-aqueous barrier, and blood-retinal barrier (Gaudana et al., 2010), as well as elimination mechanisms (e.g. tear drainage, rapid tear turnover, and reflex blinking) (Ameeruzzafar et al., 2014). These barriers can protect it against external invasion on the one hand (Jung & Chauhan, 2012; Xu et al., 2018; Liu et al., 2019), but they result in a low bioavailability of eye drops on the other hand (Rupenthal, 2017; Khan et al., 2018). The main obstacle to ocular administration is the corneal epithelium (Mannermaa et al., 2006) and the relative impermeability of the drug to the corneal epithelial membrane (Ameeruzzafar et al., 2016). The corneal epithelium, comprising non-keratinized stratified squamous cells, is $\sim 50 \mu\text{m}$ thick (Ehlers et al., 2010). It generally comprises of 5–6 layers of regularly arranged cells, including basal columnar cells in the

CONTACT Dongzhi Hou  houdongzhi406@163.com Guangdong Pharmaceutical University, Guangzhou Higher Education Mega Center, 280 Wai Huan Dong Road, Guangzhou, 510006, China; Huaqing Lin  huaqing_@163.net College of Pharmacy, Guangdong Pharmaceutical University, Guangzhou 510006, China
*These authors contributed equally to this work.

© 2021 The Author(s). Published by Informa UK Limited, trading as Taylor & Francis Group.

This is an Open Access article distributed under the terms of the Creative Commons Attribution-NonCommercial License (<http://creativecommons.org/licenses/by-nc/4.0/>), which permits unrestricted non-commercial use, distribution, and reproduction in any medium, provided the original work is properly cited.

deep layer, polyhedral cells in the intermediate layer of polyhedral cells, and squamous and polygonal-shaped cells in the surface layer (Kaur & Smitha, 2002; Jia et al., 2016). The cells are intertwined with desmosomes, band-like tight junctions, and gap junctions (Meek & Knupp, 2015), which act as a barrier to prevent the entry of materials into epithelial cell gaps and deeper tissues and inhibit their passage through the epithelium (Gaudana et al., 2010).

Medications to reduce IOP generally include carbonic anhydrase inhibitors, β -blockers, sympathomimetic drugs, and prostaglandin analogs (Pfeiffer et al., 2013; Cohen et al., 2014). Betaxolol hydrochloride (BH), an epinephrine receptor antagonist (Franc, 1987), and a retinal neuroprotectant commonly applied in glaucoma treatments (Osborne et al., 1997; Melena et al., 2000), is typically chosen as a model drug. BH can inhibit the formation of aqueous humor, dilate blood vessels, lower IOP, and improve blood circulation in the retinal optic nerve papilla (Buckley et al., 1990).

Montmorillonite (Mt) is a widely available and inexpensive layered silicate composed of tetrahedral silicon and octahedral aluminum sheets (Radmanesh et al., 2019; Xu et al., 2020). Due to its properties, such as a high surface area, two-dimensional structure, and negative charge (Dardir et al., 2018), Mt is often used in combination with polymers to create nanocomposites with improved properties (Rhee et al., 2005). BH can not only be adsorbed on the surface of Mt but also be exchanged with intercalated Na^+ to generate Mt-drug complex (Mt-BH) carriers (Zhao et al., 2019). Eudragit polymers are a type of ammonium methacrylate copolymer with permeabilities and release parameters that can be conveniently adjusted by changing the proportions of the Eudragit RS/RL mixtures (Singh et al., 2011; Saharan et al., 2019).

To reduce the frequency of administration and maintain an effective drug concentration at the target site for a longer period of time, cationic BH drug molecules were embedded in negatively charged montmorillonite by an ion-exchange reaction and then encapsulated with the skeleton materials Eudragit RS and Eudragit RL to prepare MIDFDS (Tian et al., 2018). In tear film, the hydrophilic glycocalyx of mucin forms a hydrogel network, and the sialic acid ($\text{pK}_a = 2.6$) and sulfonic acid residues in mucin are negatively charged (Gipson & Argüeso, 2003; Ablamowicz & Nichols, 2016), thus forming a polyacrylic material. A polyacrylic resin material with a positive charge, prepared by Eudragit microspheres coupled with an ion-exchange function embedded with Mt, was therefore designed to enhance the micro-interaction mechanism and further prolong precorneal retention.

Betoptoc eye drops, a microsphere suspension of BH, are currently a commonly used commercial preparation for treating glaucoma in the clinic. To expand and promote our previous work, this paper focuses on microspheres with dual functions prepared by Eudragit RS/RL and Mt, which show improved *in vivo* and *in vitro* release performance. The differences in the *in vivo* and *in vitro* physicochemical features and properties between this microsphere system and the commercial preparation Betoptoc were systematically compared and optimized, such as the particle size, pH/osmotic

pressure value, XPS, rheology, and release performance, especially the surface tension and contact angles. The performance and related mechanisms were further evaluated based on ocular irritation, *in vivo* ocular permeation, and aqueous humor pharmacokinetic and pharmacodynamic analyses.

2. Materials and methods

2.1. Materials

Mt was purchased from Zhejiang Sanding Co., Ltd. (Shaoxing, China). BH (GC >99%) was purchased from Haohua Industrial (Shandong, China). Eudragit RS PO and Eudragit RL PO (pharmaceutical adjuvants) were purchased from Degussa (Germany). 3-(4-5-Dimethylthiazol-2-yl)-2,5-diphenyltetrazolium bromide (MTT) was obtained from Amresco (USA). Betoptoc eye drops were purchased from Novartis Pharma NV (Belgium). All other reagents and solvents used were of analytical grade.

New Zealand white rabbits of either sex (SCXK 2016-0041), weighing 1.5–2.0 kg, were purchased from the Southern Medical University Laboratory Animal Center (Guangzhou, China), and all animal experiments were conducted by the Institutional Animal Care and Use Committee of Guangdong Pharmaceutical University. The human corneal epithelial (HCE) cell line was provided by the Beijing Beinaichuanlian Institute of Biotechnology Mall branch.

2.2. Manufacture of MIDFDS

MIDFDS was prepared by the patent-authorized oil-in-oil (O/O) emulsion–solvent evaporation method based on our previous study (Tian et al., 2018). Briefly, the internal phase was composed of 200 mg of Eudragit (EUD) RS PO, 200 mg of EUD RL PO, 124 mg of Tween 80, 80 mg of glycerin, 80 mg of triethyl citrate, and 50 mg of BH as Mt-BH in acetonitrile. The external phase was a mixture of 248 mg of Span 80 and 20 mL of light liquid paraffin. First, the internal phase was suspended and added to the external phase dropwise and immediately placed in an ice water bath for ultrasonication for 15 min (working power of 53%). After the mixture was stirred at room temperature until it became clear, the speed was adjusted to 650 rpm and sequentially stirred for 1 h. Finally, the microspheres were washed with hexane, collected by suction filtration, and dried naturally.

2.3. Characterization of the MIDFDS and Betoptoc

2.3.1. Particle size

The particle size of the microspheres and Betoptoc was measured by dynamic light scattering (Delsa Nano C particle size and zeta potential analyzer; Beckman Coulter, Brea, CA, USA).

2.3.2. Osmolarity and pH measurements

The osmotic pressure of MIDFDS and Betoptoc was measured with an osmometer (Osmomat Basic 3000, GonotecGmBTH, Germany), and their pH values were measured with a pH

meter (PHS-3C, INESA Scientific Instrument Co, Ltd.). The measurement results are the average value of the data obtained triplicate measurements under the same conditions.

2.3.3. Drug loading rate and encapsulation efficiency

Twenty milligrams of MIDFDS powder were dissolved in 1 mL of methylene chloride solution and vortexed for 4 min. Methanol was added to dilute to volume followed by 2 h of ultrasonic treatment and leaving at room temperature overnight to allow the microspheres to completely demulsify. The absorbance value of free BH from the filtrate after centrifugation was analyzed with an ultraviolet spectrophotometer (UV-1800, Shanghai Mapada Instruments Co., Ltd., China) at 273 nm. Betoptic (0.5 mL) was separately treated with chlorine, methanol, and dimethyl sulfoxide (DMSO) in a 100 mL volumetric flask, completely demulsified by ultrasound for 2 h and filtered through a 0.22 μm filter membrane for absorbance measurement. Next, 2 mL of MIDFDS suspension and Betoptic was placed in a dialysis bag with a molecular weight cutoff of 8,000 to 14,000 Da. Artificial tears (250 mL) were used as the dialysis medium for 30 min. The absorbance of Betoptic was determined after filtration (0.22 μm). The drug loading rate (DL%) and encapsulation efficiency (EE%) were calculated using the formulas as follows:

$$\text{EE (\%)} = \frac{D_t - D_f}{D_t} \times 100$$

$$\text{DL (\%)} = \frac{D_t - D_f}{D_t} \times 100$$

where D_t is the total amount of the drug encapsulated and unencapsulated in microsphere preparations, D_f is the amount of free drug, and D_t is the total amount of microspheres.

2.3.4. X-ray photoelectron spectroscopy (XPS)

XPS measurements were measured using a K-alpha X-ray photoelectron spectrometer (Thermo Fisher Scientific, UK) with a monochromatic Al K α X-ray source (excitation energy = 1468.6 eV). The chamber of XPS analysis was evacuated to ultra-high vacuum (pressure is $\leq 5 \times 10^{-8}$ mbar) before analysis. Spectra were collected from 0 to 1350 eV using an X-ray spot size of 400 μm with a pass energy of 100 eV for wide scan and 30 eV for individual elements. The binding energy was corrected signal at 284.8 eV relative to the carbon 1s.

2.3.5. Rheology

Rheology was proposed by Bingham and Crawford to represent the flow of liquids and the deformation of solids. Viscosity represents the resistance of the flow of a fluid. The greater the viscosity, the greater the resistance. The rheological behavior of Betoptic and MIDFDS was measured at 34 $^{\circ}\text{C}$ with a shear rate of 0–200 s^{-1} using a rotational rheometer (Physica MCR301, Austria) with a coaxial cylinder system. In addition, the dynamic viscoelasticity was measured at a frequency of 1–10 Hz. The Ostwald-de Waele power law

equation was used to fit the rheological curves of MIDFDS and Betoptic.

$$\tau = K \dot{\gamma}^n$$

where K is the viscosity coefficient of the fluid and n is the non-Newtonian index of the fluid.

2.3.6. In vitro release studies and morphological changes

The dynamic dialysis method was used for the *in vitro* release test. After preparing artificial tears (Ceulemans & Ludwig, 2002) according to the appropriate composition, the dialysis bag (molecular weight cutoff: 8000–14,000 Da) was soaked in the artificial tears overnight.

Accurately measured 4 mL of BH solution, the Betoptic eye drops and MIDFDS suspension containing the same amount of drug were packed in dialysis bags sealed at both ends and soaked in 100 mL of artificial tears. The above whole samples were placed in an air bath constant temperature oscillator with a temperature of 34 $^{\circ}\text{C}$ and a rotation speed of 120 rpm. At specific time intervals, 5 mL of the medium was pipetted out while replenishing with the same volume of freshly prepared medium (Ablamowicz & Nichols, 2016). The absorbance value of the subsequent filtrate of the removed medium filtered through a 0.22 μm microporous membrane was analyzed by an ultraviolet spectrophotometer (UV-1800, Shanghai Mapada Instruments Co., Ltd., China) at 273 nm.

For the morphological analysis, microspheres were collected at a specific time for filtration and drying. The lyophilized microspheres were fixed with double-sided carbon tape and sprayed with a thin layer of gold under a vacuum. The surface of MIDFDS was investigated using a Carl Zeiss Sigma 300 scanning electron microscope (Carl Zeiss, Germany).

2.3.7. Wettability and surface tension experiment

The eyeballs of rabbits from healthy New Zealand white rabbits were stored in 0.9% saline, and the contact angle was measured with an optical contact angle measuring instrument using the hanging drop method. BH solution, Betoptic suspension, and MIDFDS suspension were dropped into different eyeballs, and the instant image of the sample solution contacting the cornea was recorded with a camera. The measurement of surface tension was photographed at the instantaneous state of each sample solution as it dripped away from the syringe needle. Both images were analyzed using image analysis software.

2.4. In vivo fluorescence tracing

The BH solution, Betoptic suspension, and MIDFDS suspension were mixed with 0.2% sodium fluorescein. Nine healthy New Zealand white rabbits were randomly divided into three groups. A 50 μL sample (BH solution, Betoptic suspension, and MIDFDS suspension) was dripped into the lower conjunctival sac of each rabbit's eye, and a slit fluorescent lamp was used to observe and record the intensity of the

continuous fluorescent layer on the corneal surface at regular intervals (Ablamowicz & Nichols, 2016).

2.5. Aqueous humor pharmacokinetics by microdialysis

The rabbits were randomly divided into three groups: the BH solution group, the commercial Betoptic group, and the MIDFDS suspension group. Heparin sodium (100 U/kg) was injected into the ear vein of the rabbits 4 or 0.5 h before application of the drug. Rabbits were anesthetized by intravenous injection of 3% pentobarbital sodium (30 mg/kg). After local anesthesia with a drop of Benoxil on the corneal surface, the rabbit was fixed on the dissecting table, and its eyelid was opened with an eyelid opener. A penetrating puncture was performed at the edge of the cornea and sclera with a 1 mL syringe needle. After the microdialysis probe was pierced along the needle cavity, the needle was removed, and the position of the probe was adjusted so that the probe was immersed in the aqueous humor. After the probe was fixed in the corner of the eye with tissue glue, the eye was closed, and the rest of the probe was fixed on the rabbit body. Ofloxacin eye drops were dropped into the wound to prevent infection. Normal saline was used as the perfusion solution, and the flow rate was set to 2 μ L/min. After 2 h of flushing, the corresponding dosage form was given into the conjunctival sac of each group (50 μ L each time, twice in 1 min). The time of completion of administration was 0, and samples were collected every 30 min for 10 h. The collected samples were stored in a 4 °C refrigerator, and the determination was complete within 24 h (Wei et al., 2006; Gan et al., 2010).

2.6. Pharmacodynamics

Healthy rabbits were given 50 μ L of BH solution, Betoptic or MIDFDS in the left eye conjunctival sac, and the drug was gently pressed into the nasolacrimal duct; their right eyes were given the same volume of 0.9% saline. The IOP of both eyes was measured at specific time intervals, and the average value was determined from three measurements.

2.7. Ocular biocompatibility

2.7.1. Cytotoxicity

The 3-(4,5-dimethylthiazol-2-yl)-2,5-diphenyltetrazolium bromide (MTT, Amresco, USA) assay was used to evaluate the cytotoxicity of Betoptic and MIDFDS on corneal epithelial cells *in vitro*. HCE-T cells were inoculated in the culture medium in 96-well plates and treated with the specified concentration of compounds for 0.5, 2, or 4 h. Then, 100 μ L of MTT solution (5 mg/mL) was added followed by incubation for another 4 h. The absorbance at 570 nm was measured with a Multiskan™ FC Microplate spectrophotometer (Thermo Fisher Scientific, USA) (Ablamowicz & Nichols, 2016).

2.7.2. Hemolysis experiment

Irritating chemicals can cause erythrocyte membrane damage and lead to hemoglobin leakage; therefore, the content of oxygenated hemoglobin was quantified by hemolysis to evaluate the damage effects on the eye tissue of the subjects. Blood samples (2 mL) from the ear veins of healthy rabbits were gently stirred, and 2 mL of PBS was added. After centrifugation for 5 min, the supernatant was discarded. Ten milliliters of PBS were continuously added, and after 5 min of centrifugation, the supernatant was discarded. The above operation was repeated 4–5 times until the supernatant was without an obvious red color. The resulting red blood cells were diluted with PBS to form a red blood cell suspension with a volume fraction of 2%. PBS (negative control group), deionized water (positive control group), and Betoptic and MIDFDS (sample groups to be tested) were added to 0.2 mL of the erythrocyte solution, incubated at 37 °C for 4 h and centrifuged for 5 min. The supernatant color was observed. From each group, 100 μ L of the supernatant was placed in a 96-well plate, the absorbance was measured with an enzyme marker (570 nm), and the hemolysis rate was calculated (Ablamowicz & Nichols, 2016).

2.7.3. Draize test and histopathology examination

The Draize test and histopathology examinations were used to examine the irritation and ocular toxicity of the ocular tissue level *in vivo*. Preparations were directly dripped into the conjunctival sac of each rabbit's left eye, with the contralateral eye serving as a control. In the single stimulation test, 50 μ L of each drug was administered once, while in the multiple stimulation test, 50 μ L of each drug was administered three times each day for 7 consecutive days. The ocular condition (corneal lesions, iris, conjunctival congestion, edema, and secretions) was monitored using a scoring system (Jin et al., 2018) at 1, 24, 48, and 72 h after administration as previously stated. The histopathological examination was carried out following the Draize test after multiple administrations. The excised eyeballs, fixed in 10% formalin solution (v/v), were stained and observed under a microscope (BK6000, Chongqing Optec Instrument Co., Ltd.).

2.8. Statistical analysis

All statistical analyses were performed using Origin 2018 software, followed by Tukey's honestly significant difference (HSD) test for multiple comparisons in Prism 8.0 (GraphPad Software). Comparisons with *p*-values <.05 were considered statistically significant and are marked with an asterisk. All data are expressed as the mean \pm standard deviation (SD).

3. Results and discussion

3.1. Characterization of the MIDFDS and Betoptic

The physicochemical characteristics of Betoptic and MIDFDS are summarized in Table 1. Betoptic was $\sim 2.25 \pm 0.06 \mu$ m, and MIDFDS possessed a larger particle size of $9.64 \pm 3.06 \mu$ m. The particle size of ophthalmic microspheres is usually

Table 1. Physicochemical characteristics of Betoptic and MIDFDS (data expressed as the mean values \pm SD, $n = 3$).

Samples	Particle size (μm)	EE%	DL%	pH	Osmolarity (mOsmol/kg)
Betoptic	2.25 ± 0.06	61.79 ± 0.69	1.42 ± 0.09	7.11 ± 0.01	295.67 ± 1.21
MIDFDS	9.64 ± 3.06	82.03 ± 1.21	6.55 ± 0.12	6.74 ± 0.02	342.33 ± 1.33

**Figure 1.** Schematic diagram of the preparation process of MIDFDS using the oil-in-oil emulsion evaporation method.

controlled at ca. $10 \mu\text{m}$, because a larger particle would produce a foreign body sensation after microsphere entry into the eye (Liu et al., 2019). In this case, both Betoptic and MIDFDS met the particle size requirements for clinical drug compliance of ophthalmic preparations. The pH has an impact on the comfort, safety, stability, and activity of ophthalmic products. The pH of normal tears is ~ 7.4 , and ocular preparations with a pH in the range of 6–8 may not cause discomfort (Kang et al., 2016). Therefore, the pH values of MIDFDS and Betoptic were controlled at ca. 6.74 and 7.11, respectively. The osmolarity of Betoptic was ~ 295.67 mOsmol/kg, which was within the tolerance range values of the eye (248–371 mOsmol/kg). We adjusted the osmolarity of MIDFDS to 342.33 ± 1.33 mOsmol/kg with 4.5% mannitol solution to minimize irritation with the application of the eye drops. It is very interesting to note that the BH encapsulation efficiency of the MIDFDS (82.03 ± 1.21) increased compared with that of the commercial preparation Betoptic (61.79 ± 0.69). The drug loading of MIDFDS ($\sim 6.5\%$ w/w) was even 4.53 times higher than that of Betoptic ($\sim 1.4\%$ w/w), demonstrating that MIDFDS could load a sufficient amount of drug and meet the clinical dose. The drug load and entrapment efficiency of Betoptic microspheres were limited.

Therefore, a large number of free BH molecules exist in the suspension, which can be confirmed by the notable burst release observed in the *in vitro* release curve (Figure 3(b)). As a result, we were concerned about the appropriateness of using microspheres stored in liquid form for drug delivery. Considering the water-soluble properties of BH, the microspheres and buffer should be packed separately, and the mixing method should be more beneficial for clinical drug delivery.

3.1.1. X-ray photoelectron spectroscopy (XPS)

X-ray photoelectron spectroscopy (XPS) is a powerful tool for characterizing the surface of polymers (Davies et al., 1989), and provides qualitative and quantitative information about the chemical composition with a penetration depth of ~ 10 nm (Saboo et al., 2019; Sun et al., 2021). The full XPS spectrum of the samples revealed that BH was loaded on the montmorillonite and coated with Eudragit to form the dual-functioning sustained-release carrier of MIDFDS (Figure 2(c)). The XPS of Mt-BH displayed a distinct peak at 398.4 eV, which indicated that the presence of N 1s might result from BH loaded on montmorillonite (Figure 2(d)).

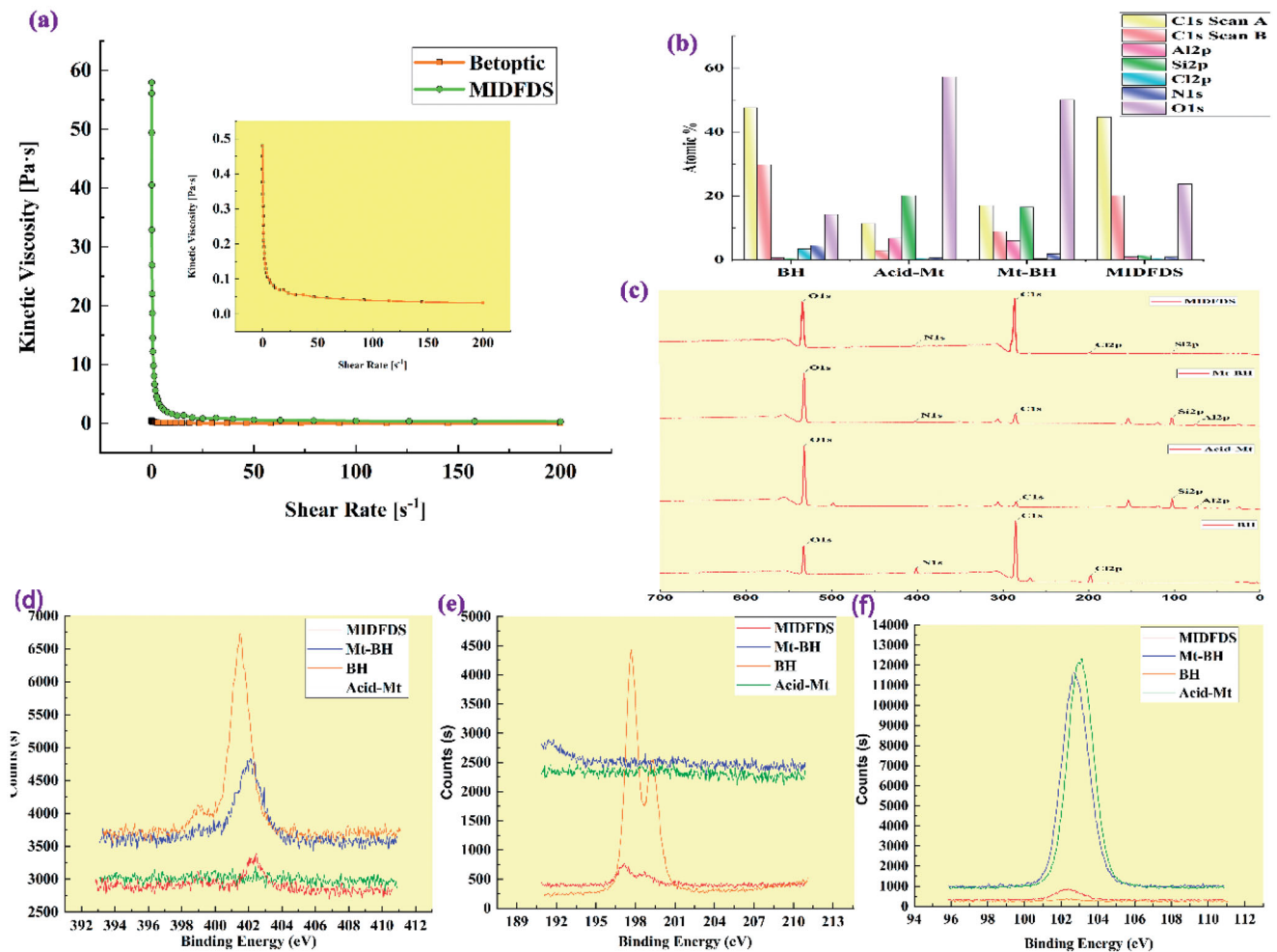


Figure 2. Characterization of MIDFDS and Betoptoc. (a) Viscosity of Betoptoc and MIDFDS at 34 °C as a function of the shear rate. (b) XPS atomic concentrations of BH, Acid-Mt, Mt-BH, and MIDFDS. (c) X-ray photoelectron full spectrum of BH, Acid-Mt, Mt-BH, and MIDFDS. (d) The N 1s XPS spectrum of BH, Acid-Mt, Mt-BH, and MIDFDS. (e) The Cl 2p XPS spectrum of BH, Acid-Mt, Mt-BH, and MIDFDS. (f) The Si 2p XPS spectrum of BH, Acid-Mt, Mt-BH, and MIDFDS.

Moreover, in the Cl 2p XPS spectrum (Figure 2(e)), Mt-BH did not show a characteristic peak at 197 eV, which further confirmed that BH was embedded on the montmorillonite by replacing Na⁺ via the ion-exchange mechanism. The XPS spectrum of Mt and Mt-BH had obvious peaks at 102.6 eV corresponding to Si 2p, while MIDFDS had a soft peak (Figure 2(f)). This finding suggested a significantly reduced Si content on the surface of the microspheres (Figure 2(b)). Together with the X-ray diffraction (Tian et al., 2018), Mt-BH was mainly distributed in deeper areas of the MIDFDS rather than adsorbed on the surface.

3.1.2. Rheology

Pseudoplastic flow, plastic flow, and thixotropic flow behavior can effectively slow down the sedimentation speed of sub-particles in suspension. The Ostwald-de Waele power law equation was used to fit the rheological curves of the remaining MIDFDS and Betoptoc (Table 2). The fitting results showed that the samples were shear-thinning pseudoplastic non-Newtonian fluids ($n < 1$), which have the advantage of remaining on the ocular surface. The smaller the value of the non-Newtonian index, the more significant the non-Newtonian characteristics. Combined with Figure 2(a), it

could also be confirmed that Betoptoc showed only slight pseudoplastic behavior. Conversely, MIDFDS showed a high initial viscosity when the shear rate was below 10 s⁻¹, indicating that their retentivity was superior to that of Betoptoc at rest when the eye was open. Then, the viscosity decreased rapidly with the increase in shear rate. As the shear rate exceeded 200 s⁻¹, the viscosity reached its minimum, which was extremely low. Thus, under the shear of the eyelid (5000 s⁻¹), MIDFDS, as well as Betoptoc, would demonstrate low viscosity, which could avoid irritation and discomfort (Destruel et al., 2020).

3.1.3. In vitro release studies and morphological changes

Currently, the purpose of drug delivery research is to develop systems to maintain the drug concentration between the minimum effective level and the maximum safe level over a long period of time. The *in vitro* release curves of the BH solution, Betoptoc, and MIDFDS are shown in Figure 3(b). Unexpectedly, both BH solution and Betoptoc had comparatively high burst release characteristics within 0.5 h with releases of 58.40 and 51.43%, and the drug in each sample was completely released within 3 h vs. BH solution within 2 h. Thus, the commercial suspension Betoptoc

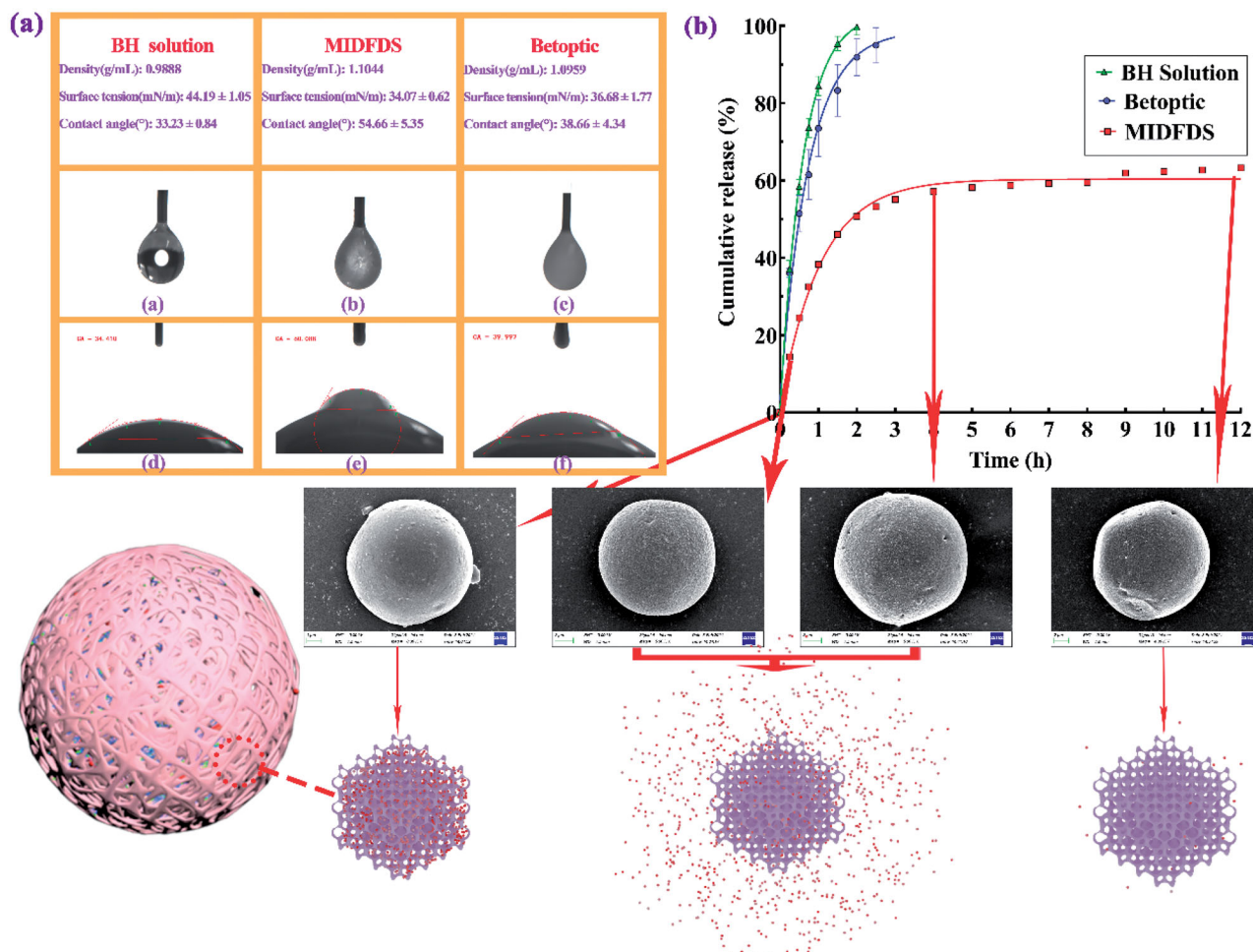


Figure 3. Surface tension and contact angle values of the BH solution, Betoptic, and MIDFDS (data expressed as the mean values \pm SD, $n=3$). 1–6 are one-time measurement results. (a) *In vitro* cumulative release percentage curve of BH solution, Betoptic, and MIDFDS ($n=3$), and SEM images of MIDFDS at 0, 0.5, 4, and 12 h. (b) The drug was released from the core of the microsphere through the pore formed by the swelling of Eudragit in MIDFDS following Fick diffusion without dissolved MIDFDS.

and BH showed considerable release performance *in vitro*, although it did not meet the requirements of the Chinese Pharmacopoeia that the release of sustained-release preparations within 0.5 h should be $<40\%$. In contrast, MIDFDS showed a release rate of 24.48% within 0.5 h, which is a relatively low burst release phase, and they were continuously released for 12 h. Based on these results, we concluded that the inorganic-organic compound sustained-release system formed by specific ion-exchanged Mt and Eudragit RS/RL (MIDFDS) could exhibit the above double-sustained and controlled release effects. Hence, MIDFDS displayed key superiority in its minimal initial burst release and complete steady sustained release, providing a beneficial therapeutic window and decreasing the dosing frequency in the clinic (Liu et al., 2019).

With a prolonged incubation time in the release medium, the volume of the microspheres began to increase. Subsequently, an increasing number of pores appeared on the microsphere surface, and the pore size gradually increased, although the microspheres did not obviously collapse. Therefore, the release mechanism of MIDFDS can be described as follows: due to the permeability of Eudragit to water and the formation of water-absorbing swelling energy,

water molecules can enter the microsphere via the pore through the capillary effect. The drug can also gradually dissolve out from the core of the microsphere via the pore according to Fick diffusion ($n=0.2207$). The drug was replaced from the surface and interlayer of montmorillonite by ion exchange with K^+/Na^+ in the tear film and then diffused and dissolved onto the surface of the microsphere. This phenomenon also explains why the MIDFDS could basically maintain a spherical shape following release *in vitro* for 12 h.

3.1.4. Surface tension and contact angle

Surface tension is the unbalanced force of surface molecules, causing surface molecules to be pulled into liquid due to their elastic tendency. The lower the surface tension of the preparation, the easier it is for the corneal epithelium to moisten. The BH aqueous solution, Betoptic, and MIDFDS showed low surface tensions, supporting their suitable diffusion abilities and corneal permeability.

The contact angle is usually used to reflect the degree of wettability of liquid on a solid surface. The smaller the contact angle, the greater the wetting degree of the preparation

Table 2. Rheological behavior of Betoptic and MIDFDS ($n=3$).

Formulation	Power law equation	Non-Newtonian index (n)	Correlation coefficient (r)	Fluid type
Betoptic	$\tau = 0.205\dot{\gamma}^{0.626}$	$0.626 < 1$	0.9986	Pseudoplastic fluid
MIDFDS	$\tau = 10.36\dot{\gamma}^{0.265}$	$0.265 < 1$	0.9716	Pseudoplastic fluid

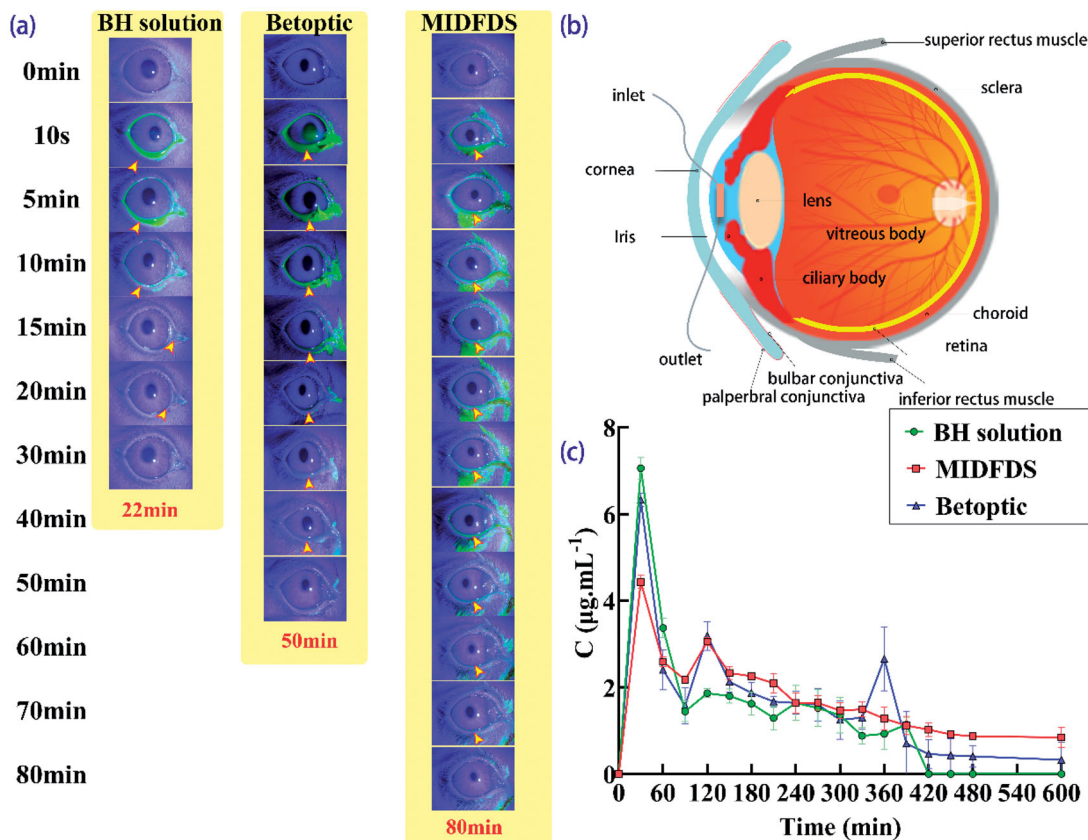


Figure 4. *In vivo* fluorescence tracing and microdialysis results. (a) Precorneal retention following the administration of BH solution, Betoptic, and MIDFDS at the specified time points. (b) Schematic diagram of a microdialysis probe implanted into the anterior chamber. (c) *In vivo* pharmacokinetic data of the BH solution, Betoptic, and MIDFDS after topical instillation into rabbit eyes (mean \pm SD, $n=3$).

on the cornea, and the better the spread ability and the faster the spreading speed. Figure 3(a) shows that the contact angle of drug-loaded microspheres ($54.66 \pm 5.35^\circ$) was significantly larger than those of Betoptic ($38.66 \pm 4.34^\circ$, $p < .05$) and BH aqueous solution ($33.23 \pm 0.84^\circ$, $p < .01$). Therefore, MIDFDS spread more slowly than Betoptic microspheres, suggesting a longer micro-interaction time of the microparticles with tear film compared with the other samples.

3.2. In vivo evaluation

3.2.1. Precorneal retention time

As shown in Figure 4(a), as expected, during the first 20 min following administration, there was almost no fluorescent residue on the corneal surface of the BH group, indicating that the retention time of BH on the eyeball surface was very short. A huge variability in all samples was observed during the first 20 min due to a large amount of preparation instilled. Upon dropping $7 \mu\text{L}$ (Van Haeringen, 1981) and $50 \mu\text{L}$ of tear fluid on the ocular surface of rabbit eyes, rapid elimination of the excess was observed in both cases either by nasolacrimal drainage or lacrimation. For the MIDFDS

group, the fluorescence was concentrated in the conjunctival sac after administration. A longer retention time on the eyeball surface was obtained compared with that of Betoptic ($p < .05$), potentially due to the larger contact angle of MIDFDS, which enables the MIDFDS to diffuse slowly on the cornea, thus MIDFDS had more time to interact with the mucin of the tear film, resulting in a longer anterior corneal retention time.

3.2.2. Aqueous humor pharmacokinetics

In this study, the microdialysis online sampling technique was used to evaluate the pharmacokinetics of the aqueous humor. The BH concentrations of BH solution, Betoptic, and MIDFDS in the rabbit aqueous humor are shown in Figure 4(b). Betoptic showed a sharp and strong drug concentration peak ($6.33 \mu\text{g}/\text{mL}$) in the aqueous humor at 30 min, which was only slightly lower than that of BH solution ($7.06 \mu\text{g}/\text{mL}$). This phenomenon was due to the rapid release of free drugs or drugs adsorbed onto the surface of the Betoptic microspheres, which could be confirmed by the measured entrapment efficiency of Betoptic (only 61.79%) and a fast and sudden burst release *in vitro* (Figure 3(b)). After 30 min, the

drug concentration of all samples began to decrease because the drug overflowed from the conjunctival sac or was lost through nasolacrimal drainage. The decreases in BH solution and Betoptic were more significant than that of MIDFDS. Thus, the fluctuation in the drug concentration of MIDFDS was less dramatic than that of the former two. MIDFDS showed the most stable pharmacokinetics and greatest drug release performance (except for occasional sudden release points, $p < .05$) in the aqueous humor among the three preparations, favoring their stable and reliable pharmacodynamic IOP-lowering effects.

3.2.3. Pharmacodynamics

The IOP-lowering efficacy measurements indicated that BH solution reached its maximum IOP reduction capacity at 1 h, gradually weakened after 2 h, and then had no effect at 4 h. The effects of MIDFDS and Betoptic on lowering IOP were better than those of BH solution, except at 1 h. The BH solution had an extremely rapid IOP-lowering effect due to the rapid release of the solution. The Betoptic curve fluctuated considerably, especially during the two intervals of 1.5–3.0 and 3.0–8.0 h, which could be attributed to a large amount of free drug adsorbed on the surface of Betoptic microspheres. Although Betoptic appeared to have a larger IOP reduction than MIDFDS, its significant fluctuations could reduce the clinical compliance of patients and in turn contributed to an adverse impact on the intraocular tissue. Of the three curves, MIDFDS had the smoothest IOP-lowering effects. It is worth noting that MIDFDS still had a continuous IOP-lowering effect after 8 h, which was much longer than that of Betoptic.

Generally, the precorneal fluorescence retention time of the MIDFDS (90 min) was longer than that of Betoptic (70 min). Except for a few points, the overall aqueous humor pharmacokinetic curve of the MIDFDS was generally higher than that of Betoptic, with longer-lasting pharmacodynamics of lowering IOP. The improved aqueous humor pharmacokinetics and pharmacodynamics of the MIDFDS probably resulted from the longer precorneal fluorescence retention. The above measurements of the corneal contact angle tests showed that MIDFDS had the largest contact angle (54.66 ± 5.75); however, they had a slower corneal spreading rate (2.93 s) than that of Betoptic microspheres (2.50 s, [Figure 5\(a\)](#)). The slow wetting and diffusion of the MIDFDS on the ocular surface enabled a longer interaction time between the positively charged microspheres (ζ potential of $+8.24 \pm 3.98$ mV) and the negatively charged sialic acid and sulfonic acid residues in the tear film. Therefore, more MIDFDS was trapped in front of the cornea by a mucin gel network in the lacrimal film, and the corresponding macroscopic manifestation was a prolongation of the fluorescence retention in the rabbit cornea.

MIDFDS had a longer retention time than Betoptic but a poorer cumulative release percentage. Surprisingly, MIDFDS still resulted in much higher aqueous humor concentrations and longer-lasting efficacy. The tear film is located in front of the cornea, and it contains a variety of sialic acid and sulfonic acid residues, lysozyme-based coenzymes, and different

distributions of sialic acid and sulfonic acid residues ($pK_a = 2.6$), which might lead to a much lower pH near the cornea than the average pH value of the tear film water layer (Murgia et al., 2016; Ahmed et al., 2018). Tear film ranges in pH from 6.5 to 7.6 (Moreddu et al., 2020). These observations suggested that the pH of residues and other coenzymes in tears could promote the degradation and drug release of microspheres. Therefore, the lysozyme release experiment was performed, and the results ([Figure 5\(c\)](#)) showed no significant effect of lysozyme on release at 34°C ($p > .05$). Next, the influence of different pH values on MIDFDS release was examined, and [Figure 5\(d\)](#) shows that a lower pH of the release medium resulted in faster and more complete release of MIDFDS compared with $pH = 7.4$ ($p < .001$), with the faster and more complete release of $80.87 \pm 3.83\%$ obtained at $pH = 6.5$ which had no significant difference to $pH = 2.6$. Therefore, compared with Betoptic, MIDFDS suspension eye drops had the ability to maintain a stable drug concentration for a long time. Both the sustained release of MIDFDS based on the ion-exchange mechanism and the sufficient pre-corneal retention time contributed to a sufficient and stable drug concentration in the aqueous humor. Together with the above findings, these results demonstrate a more stable and long-term reduction of IOP with the dual-functioning sustained-release carrier of MIDFDS.

3.3. Ocular biocompatibility

Although the MIDFDS demonstrated potential therapeutic applications through pharmacodynamic analyses, its clinical application safety remains a concern. We explored the cytotoxicity and undertook an *in vitro* hemolytic study, a histology study, and a Draize test to evaluate their safety profile.

3.4.1. Cytotoxicity

The first parameter considered for application to a target material is to evaluate the cytotoxicity of any substance that comes in contact with the eye surface. The cytotoxicity of human corneal endothelial cells was evaluated *in vitro* by the MTT assay using human corneal epithelial cells (HCECs). With the increase in the preparation concentration, the survival rate of HCECs decreased. Except for the highest dose (100 μL), the cell survival rates of MIDFDS were all higher than those of Betoptic. The Occupational Safety and Health Administration (OSHA) states that the accepted proportion of cell viability is expected to be higher than 70%. The MTT assay showed that when the dose was 20 μL (although the administration dosage was 50 μL , the volume would be quickly reduced due to nasolacrimal drainage), the cell viability in the MIDFDS group was 90.4, 88.4, and 75.0% after exposure for 0.5, 2, and even 4 h, respectively, which was significantly ($p < .001$) higher than in the Betoptic group (64.1, 41.1, and 42.2%, respectively). The results showed that at the clinical dose (20 μL), the biocompatibility of the homemade double-effect microspheres was better than that of the Betoptic microspheres. Through our previous studies, strong cytotoxicity of drugs (Liu et al., 2020) and weaker cytotoxicity

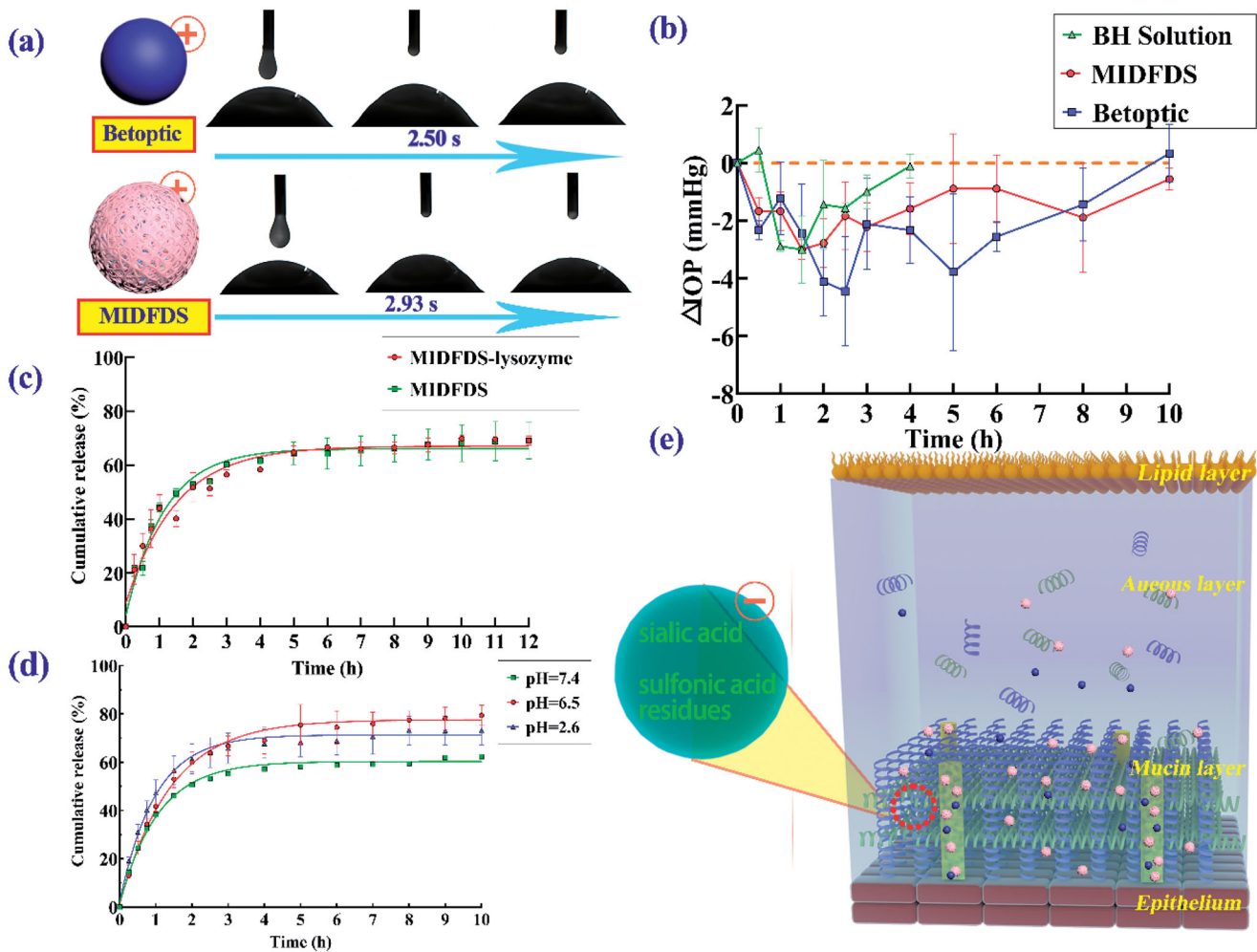


Figure 5. Pharmacodynamics and corneal preparation spread time. (a) The spreading time of Betoptic and MIDFDS at the front of the rabbit cornea *in vitro*. (b) IOP-lowering effects of topical administration of BH solution, Betoptic, and MIDFDS (mean \pm SD, $n = 3$). (c) *In vitro* release of BH from MIDFDS and MIDFDS-lysozyme ($n = 3$). (d) *In vitro* release of BH from MIDFDS at different pH values ($n = 3$). (e) Schematic diagram of the micro-interaction between the positively charged microspheres and the negatively charged mucin layer after local administration. The larger corneal contact angle of MIDFDS and the slower corneal diffusion velocity in rabbit eyes led to increased interaction time between the positively charged surface of MIDFDS and the negative residues of the tear film, further resulting in a longer precorneal retention time of MIDFDS in *in vivo* fluorescence tracing (Figure 4(a)).

of blank Eudragit microspheres (Liu et al., 2020) proved that the toxicity was mainly caused by drugs rather than carriers, which suggested that drugs were more encapsulated in the microspheres than adsorbed on the surface.

3.4.2. Hemolysis experiment

Allergy and hemolysis, which are other important components of the preclinical safety evaluation, refer to the local toxicity or systemic toxicity caused by drug administration through non-oral routes, such as skin, mucous membranes, and blood vessels (Lagarto et al., 2006). Incubation with erythrocytes indicated that the red blood cells declined in the negative control group, causing the supernatant to be colorless and transparent in the absence of hemolysis (Figure 6(e)). The positive control group showed a red clear solution, and only a small amount of red blood cells remained at the bottom of the tube, which clearly indicated hemolysis. For the MIDFDS sample group, the red blood cells declined in each tube, resulting in a colorless and transparent

supernatant without hemolysis or coagulation. Each tube of Betoptic samples was red and clear with hardly any red blood cell residue at the bottom of the tube, which was clearly caused by hemolysis. The above results showed that the MIDFDS (0.006%) caused significantly less hemolysis than the BH-PBS solution (2.74%, $p < .01$) and Betoptic (48.69%, $p < .001$), which suggested that MIDFDS with ion-exchange effects and a positively charged surface possesses excellent biocompatibility compared with Betoptic in terms of cytotoxicity and hemolysis.

3.4.3. Draize test and histopathology examination

Eye irritation is accompanied by eye blinks and increased tear secretion as a defense mechanism for the recovery of normal conditions. When confronted with these discomforts, the defense mechanism may be a more rapid loss of the drug with a reduction of the therapeutic response. The most commonly used method to evaluate eye irritation is the Draize test on rabbit eyes, which are more sensitive than

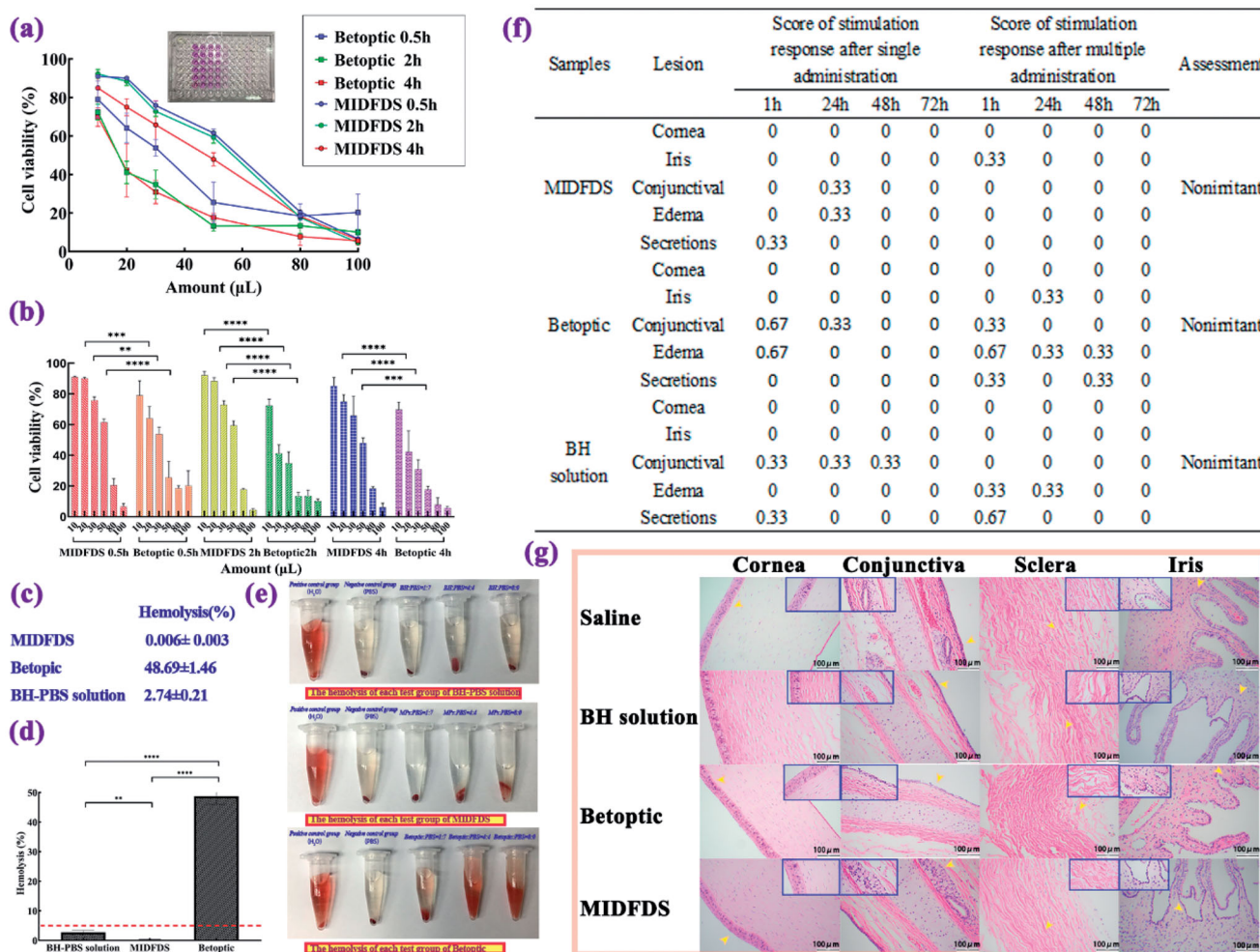


Figure 6. Biocompatibility evaluation of Betoptic and MIDFDS. (a,b) Percent cell viability of each formulation after different exposure times and administration dosages ($n = 3$, mean \pm SD). (c,d) Hemolysis percentage of the BH-PBS, Betopic, and MIDFDS. The dashed line in (d) indicates 5% hemolysis. (e) The hemolysis of each test group after 4 h of incubation with erythrocytes. (f) Ocular irritation scores from rabbits (single and multiple administrations, $n = 3$). (g) Ocular tissues were stained with hemoxilyn and eosin (H&E) following chronic application in the saline group, BH solution group, Betoptic group, and MIDFDS group (magnification 200 \times).

human eyes. Macroscopic changes were evaluated by the Draize rabbit eye test of the cornea, iris, conjunctiva, edema, and secretions of rabbit eyes after exposure to the preparations. Tissues exposed to Betoptic and MIDFDS did not show any obvious differences from those that received the saline control, because there was no edema, bleeding or inflammation detected. H&E-stained sections of ocular tissues confirmed that repeated dosing of Betoptic and MIDFDS did not alter the structure of the cornea, conjunctiva, sclera, or iris (Figure 6(g)). These results indicated that Betoptic and MIDFDS will not stimulate or damage the eye tissue and may be suitable for short-term or long-term local eye application. Although the biocompatibility of Betoptic was inferior to that of MIDFDS according to the cytotoxicity and hemolysis experiments, the difference in irritation at the cellular level was not enough to cause significant histological changes in rabbits *in vivo*. It should be noted that glaucoma treatment generally requires long-term administration; therefore, the Draize experiment in this study was performed for 72 h.

4. Conclusion

The combination of BH embedded in Mt and Eudragit was developed, and its *in vivo* and *in vitro* behavior compared with commercial Betoptic was investigated. The dual-functioning sustained-release carrier of MIDFDS demonstrated a small amount of initial burst release and persistent sustained release up to 12 h, while Betoptic was released in its entirety within only 3 h. The longer corneal spread time at the front of the cornea allowed much more time for MIDFDS micro-interactions and thus longer precorneal retention than Betoptic. MIDFDS was superior in terms of enhancing the drug concentration in the aqueous humor and was more stable overall. The pharmacokinetic results showed that MIDFDS also displayed smooth and steady IOP reduction. In addition, the MIDFDS formulations were less irritating due to reduced cytotoxicity and hemolysis. In conclusion, the dual-functioning sustained-release carrier MIDFDS could be a promising ophthalmic sustained delivery system for the treatment of glaucoma.

Acknowledgments

We acknowledge the help from the Guangdong Provincial Engineering Center of Topical Precise Drug Delivery Systems in performing the experiments.

Ethical approval

All animal experiments were conducted by the Institutional Animal Care and Use Committee of Guangdong Pharmaceutical University.

Disclosure statement

The authors report no conflicts of interest.

Funding

This work was supported by the National Natural Science Foundation of China (No. 51192052), the Science and Technology Planning Project of Guangdong Province (No. 2020B1212060055), and College Students' Innovative Entrepreneurial Training Plan Program (No. S202010573025).

Data availability statement

The datasets used and/or analyzed during the current study are available from the corresponding author on reasonable request.

References

- Ablamowicz AF, Nichols JJ. (2016). Ocular surface membrane-associated mucins. *Ocul Surf* 14:331–41.
- Actis AG, Versino E, Brogliatti B, Rolle T. (2016). Risk factors for primary open angle glaucoma (POAG) progression: a study ruled in Torino. *TOOPHTJ* 10:129–39.
- Ahmed TA, Badr-Eldin SM, Ahmed OAA, Aldawsari H. (2018). Intranasal optimized solid lipid nanoparticles loaded *in situ* gel for enhancing trans-mucosal delivery of simvastatin. *J Drug Deliv Sci Technol* 48: 499–508.
- Ameeduzzafar Ali J, Bhatnagar A, Kumar N, et al. (2014). Chitosan nanoparticles amplify the ocular hypotensive effect of catechol in rabbits. *Int J Biol Macromol* 65:479–91.
- Ameeduzzafar A, Ali J, Fazil M, et al. (2016). Colloidal drug delivery system: amplify the ocular delivery. *Drug Deliv* 23:710–26.
- Ameeduzzafar Imam SS, Abbas Bukhari SN, Ahmad J, et al. (2018). Formulation and optimization of levofloxacin loaded chitosan nanoparticle for ocular delivery: *in-vitro* characterization, ocular tolerance and antibacterial activity. *Int J Biol Macromol* 108:650–9.
- Amo EM, Urtti A. (2008). Current and future ophthalmic drug delivery systems A shift to the posterior segment. *Drug Discov Today* 13: 135–43.
- Arranz-Romera A, Davis BM, Bravo-Osuna I, et al. (2019). Simultaneous co-delivery of neuroprotective drugs from multi-loaded PLGA microspheres for the treatment of glaucoma. *J Control Release* 297:26–38.
- Buckley MMT, Goa KL, Clissold SP. (1990). Ocular betaxolol. A review of its pharmacological properties, and therapeutic efficacy in glaucoma and ocular hypertension. *Drugs* 40:75–90.
- Ceulemans J, Ludwig A. (2002). Optimisation of carbomer viscous eye drops: an *in vitro* experimental design approach using rheological techniques. *Eur J Pharm Biopharm* 54:41–50.
- Cohen LP, Pasquale LR, Crabb JW, et al. (2014). Clinical characteristics and current treatment of glaucoma. *Cold Spring Harb Perspect Med*. 4:a017236.
- Dardir FM, Mohamed AS, Abukhadra MR, et al. (2018). Cosmetic and pharmaceutical qualifications of Egyptian bentonite and its suitability as drug carrier for Praziquantel drug. *Eur J Pharm Sci* 115:320–9.
- Davies MC, Wilding IR, Short RD, et al. (1989). An analysis of the surface chemical structure of polymethacrylate (Eudragit) film coating polymers by XPS. *Int J Pharm* 57:183–7.
- Delplace V, Payne S, Shoichet M. (2015). Delivery strategies for treatment of age-related ocular diseases: from a biological understanding to bio-material solutions. *J Controlled Release* 219:652–68.
- Destruel PL, Zeng N, Seguin J, et al. (2020). Novel *in situ* gelling ophthalmic drug delivery system based on gellan gum and hydroxyethylcellulose: innovative rheological characterization, *in vitro* and *in vivo* evidence of a sustained precorneal retention time. *Int J Pharm* 574: 118734.
- Ehlers N, Heegaard S, Hjortdal J, et al. (2010). Morphological evaluation of normal human corneal epithelium. *Acta Ophthalmol* 88:858–61.
- Franc H. (1987). Analysis of the nature of antagonism of the reserpine-induced hypothermia by imipramine. *Naunyn Schmiedeberg's Archiv Pharmacol* 336:303–7.
- Gan L, Han S, Shen J, et al. (2010). Self-assembled liquid crystalline nanoparticles as a novel ophthalmic delivery system for dexamethasone: improving precorneal retention and ocular bioavailability. *Int J Pharm* 396:179–87.
- Gaudana R, Ananthula HK, Parenky A, Mitra AK. (2010). Ocular drug delivery. *AAPS J* 12:348–60.
- Geyer O, Bottone EJ, Podos SM, et al. (1995). Microbial contamination of medications used to treat glaucoma. *Br J Ophthalmol* 79:376–9.
- Geyer O, Levo Y. (2020). Glaucoma is an autoimmune disease. *Autoimmun Rev* 19:102535.
- Gipson IK, Argüeso P. (2003). Role of mucins in the function of the corneal and conjunctival epithelia. *Int Rev Cytol* 231:1–49.
- Jia L, Ghezzi CE, Kaplan DL. (2016). Optimization of silk films as substrate for functional corneal epithelium growth. *J Biomed Mater Res B Appl Biomater* 104:431–41.
- Jin Q, Li H, Jin Z, et al. (2018). TPGS modified nanoliposomes as an effective ocular delivery system to treat glaucoma. *Int J Pharm* 553: 21–8.
- Jung HJ, Chauhan A. (2012). Biomaterials temperature sensitive contact lenses for triggered ophthalmic drug delivery. *Biomaterials* 33: 2289–300.
- Kang H, Cha KH, Cho W, et al. (2016). Cyclosporine A micellar delivery system for dry eyes. *Int J Nanomed* 11:2921–33.
- Kaur IP, Smitha R. (2002). Penetration enhancers and ocular bioadhesives: two new avenues for ophthalmic drug delivery. *Drug Dev Ind Pharm* 28:353–69.
- Khan N, Ameeduzzafar Khanna K, Bhatnagar A, et al. (2018). Chitosan coated PLGA nanoparticles amplify the ocular hypotensive effect of forskolin: statistical design, characterization and *in vivo* studies. *Int J Biol Macromol* 116:648–63.
- Kumarasamy NA, Lam FS, Wang AL, Theoharides TC. (2006). Glaucoma: current and developing concepts for inflammation, pathogenesis and treatment. *Eur J Inflamm* 4:129–37.
- Lagarto A, Vega R, Vega Y, et al. (2006). Comparative study of red blood cell method in rat and calves blood as alternatives of Draize eye irritation test. *Toxicol In Vitro* 20:529–33.
- Liu S, Han X, Liu H, et al. (2020). Incorporation of ion exchange functionalized-montmorillonite into solid lipid nanoparticles with low irritation enhances drug bioavailability for glaucoma treatment. *Drug Deliv* 27: 652–61.
- Liu J, Li S, Li G, et al. (2019). Highly bioactive, bevacizumab-loaded, sustained-release PLGA/PCADK microspheres for intravitreal therapy in ocular diseases. *Int J Pharm* 563:228–36.
- Liu Y, Wang Y, Yang J, et al. (2019). Cationized hyaluronic acid coated spanlastics for cyclosporine A ocular delivery: prolonged ocular retention, enhanced corneal permeation and improved tear production. *Int J Pharm* 565:133–42.
- Mannermaa E, Vellonen KS, Urtti A. (2006). Drug transport in corneal epithelium and blood-retina barrier: emerging role of transporters in ocular pharmacokinetics. *Adv Drug Deliv Rev* 58:1136–63.
- Meek KM, Knupp C. (2015). Corneal structure and transparency. *Prog Retin Eye Res* 49:1–16.
- Melena A, Osborne NN, Chidlow G. (2000). Betaxolol, a b 1 -adrenoceptor antagonist, reduces Na⁺ influx into cortical synaptosomes by

- direct interaction with Na⁺ channels: comparison with other β -adrenoceptor antagonists. *British Journal of Pharmacology* 130:759–766.
- Moreddu R, Wolffsohn JS, Vigolo D, Yetisen AK. (2020). Laser-inscribed contact lens sensors for the detection of analytes in the tear fluid. *Sens Actuators B Chem* 317:128183.
- Murgia X, Pawelzyk P, Schaefer UF, et al. (2016). Size-limited penetration of nanoparticles into porcine respiratory mucus after aerosol deposition. *Biomacromolecules* 17:1536–42.
- O'Callaghan J, Cassidy PS, Humphries P. (2017). Open-angle glaucoma: therapeutically targeting the extracellular matrix of the conventional outflow pathway. *Expert Opin Ther Targets* 21:1037–50.
- Osborne NN, Cazevielle C, Carvalho AL, et al. (1997). *In vivo* and *in vitro* experiments show that betaxolol is a retinal neuroprotective agent. *Brain Res* 751:113–23.
- Pfeiffer N, Lamparter J, Gericke A, et al. (2013). Neuroprotection of medical IOP-lowering therapy. *Cell Tissue Res* 353:245–51.
- Radmanesh F, Rijnaarts T, Moheb A, et al. (2019). Enhanced selectivity and performance of heterogeneous cation exchange membranes through addition of sulfonated and protonated montmorillonite. *J Colloid Interface Sci* 533:658–70.
- Rhee CH, Kim HK, Chang H, Lee JS. (2005). Nafion/sulfonated montmorillonite composite: a new concept electrolyte membrane for direct methanol fuel cells. *Chem Mater* 17:1691–7.
- Rupenthal ID. (2017). Drug-device combination approaches for delivery to the eye. *Curr Opin Pharmacol* 36:44–51.
- Saboo S, Mugheirbi NA, Zemlyanov DY, et al. (2019). Congruent release of drug and polymer: a “sweet spot” in the dissolution of amorphous solid dispersions. *J Controlled Release* 298:68–82.
- Saharan P, Bahmani K, Saharan SP. (2019). Preparation, optimization and *in vitro* evaluation of glipizide nanoparticles integrated with Eudragit RS-100. *Pharm Nanotechnol* 7:72–85.
- Singh B, Bhatowa R, Tripathi C, Kapil R. (2011). Developing micro-/nanoparticulate drug delivery systems using “design of experiments”. *Int J Pharm Investig* 1:75–87.
- Sun Y, Sun X, Li X, et al. (2021). A versatile nanocomposite based on nanoceria for antibacterial enhancement and protection from aPDT-aggravated inflammation via modulation of macrophage polarization. *Biomaterials* 268:120614.
- Tham YC, Li X, Wong TY, et al. (2014). Global prevalence of glaucoma and projections of glaucoma burden through 2040: a systematic review and meta-analysis. *Ophthalmology* 121:2081–90.
- Tian S, Li J, Tao Q, et al. (2018). Controlled drug delivery for glaucoma therapy using montmorillonite/Eudragit microspheres as an ion-exchange carrier. *Int J Nanomedicine* 13:415–28.
- Van Haeringen NJ. (1981). Clinical biochemistry of tears. *Surv Ophthalmol* 26:84–96.
- Wei G, Ding PT, Zheng JM, Lu WY. (2006). Pharmacokinetics of timolol in aqueous humor sampled by microdialysis after topical administration of thermosetting gels. *Biomed Chromatogr* 20:67–71.
- Xu W, Peng J, Ni D, et al. (2020). Preparation, characterization and application of levan/montmorillonite biocomposite and levan/BSA nanoparticle. *Carbohydr Polym* 234:115921.
- Xu J, Xue Y, Hu G, et al. (2018). A comprehensive review on contact lens for ophthalmic drug delivery. *J Control Release* 281:97–118.
- Zhao Y, Li J, Han X, et al. (2019). Dual controlled release effect of montmorillonite loaded polymer nanoparticles for ophthalmic drug delivery. *Appl Clay Sci* 180:105167.